研究論文

DOI: http://dx.doi.org/10.6108/KSPE.2013.17.1.009

음속 및 초음속 노즐을 통한 Gas-Solid Suspension 유동에 대한 해석적 연구

JianGuo Sun* · G.Rajesh** · 김희동***†

Analytical Study on the Gas-Solid Suspension Flows through Sonic and Supersonic Nozzles

JianGuo Sun* · G.Rajesh** · Heuydong Kim***†

ABSTRACT

A considerable deal of work has been carried out to get an insight into the gas-solid suspension flows and to specify the particle motion and its influence on the gas flow field. In this paper an attempt is made to develop an analytical model to study the effect of nozzle inlet/exit pressure ratio, particle/gas loading and the particle diameter effect on gas-solid suspension flow. The effect of the particle/gas loading on the mass flow, Mach number, thrust coefficient and static pressure variation through the nozzle is analyzed. The results obtained show that the presence of particles seems to reduce the strength of the shock wave. It is also found that smaller the particle diameter is, bigger will be the velocity as bigger particle will have larger slip velocity. The suspension flow of smaller diameter particles has almost same trend as that of single phase flow with ideal gas as working fluid. Depending on the ambient pressure, the thrust coefficient is found to be higher for larger particle/gas loading or back pressure ratio.

초 록

Gas-solid suspension 유동에서의 입자운동과 그 운동이 유동장에 미치는 영향을 명시하고, 이 유동에 대한 이해를 얻기 위해 많은 연구가 수행 되어 왔다. 본 논문에서는 gas-solid suspension 유동에 대한 노즐의 입구/출구 압력비, 입자/기체 부하, 입자의 직경에 따른 영향 등을 연구하기 위한 분석적 모델을 개발 하였다. 노즐을 통한 유량, Mach수, 추력계수 및 정압 변화에 대한 입자/기체 부하의 영향을 분석하였다. 그 결과로부터 입자의 존재로 인해 충격파의 강도가 줄어드는 것으로 판단되며, 입자 직경이 커질수록 속도는 작아지고, slip velocity는 커지게 될 것이다. 또한, 더 작은 직경의 입자에 대한 suspension 유동은 이상기체에 대한 단상유동의 결과와 같은 경향이 나타나며, 주위 압력에 따라 더 큰 입자/기체 부하나 배압비에 대한 추력계수가 더 크게 나타났다.

Key Words: Gas-solid Flow(기체-고체 유동), Flow Choking(유동 초킹), Convergent-divergent Nozzle(축소-확대 노즐), Analytical Study(해석적 연구)

접수일 2012. 4. 2, 수정완료일 2012. 12. 11, 게재확정일 2012. 12. 17

* 학생회원, 안동대학교 기계공학과
** 정회원, 계명대학교 기계자동차공학과
*** 종신회원, 안동대학교 기계공학과
† 교신저자, E-mail: kimhd@andong.ac.kr

Nomenclature

a	speed of sound	[m/s]

a_s	speed of sound of mixture	[m/s]
C_D	drag coefficient of particle	[----]
C_v	constant pressure specific heat of gas	[J/kg·K]
C_s	specific heat of particle	[J/kg·K]
d_p	diameter of particle	[mm]
h_m	enthalpy	[J/kg]
Re_p	Reynolds number of particle	[----]
p_a	ambient pressure	[bar]
p_e	outlet pressure of nozzle	[bar]
p_0	inlet pressure of nozzle	[bar]
u_{int}	internal energy	[J/kg]
v_p	velocity of particle	[m/s]
v_g	velocity of gas	[m/s]
ρ_p	density of material of particle	[kg/m^3]
ρ_{ds}	density of dispersed particle	[kg/m^3]
ρ_g	density of gas	[kg/m^3]
ρ_f	mass of gas in unit volume	[kg/m^3]
ε	volume fraction	[----]
ρ_m	mixture density	[kg/m^3]
γ	specific heat ratio of gas	[----]
$\bar{\gamma}$	specific heat ratio of mixture	[----]
η	particle/gas loading	[----]
μ	dynamic viscosity	[N·s/m^2]
T	temperature of mixture	[K]

1. Introduction

The gas-solid suspension flows are widely encountered in national defense and industrial processes, like rockets, particulate pneumatic transport, fluidized beds etc.[1]. For high speed gas-solid suspension flow, such as those in encountered in supersonic cold gas sprays (SCGS) and needleless injectors, the velocity of suspension flow always reaches supersonic speeds[2].

Supersonic gas-solid suspension flows are always associated with lots of complex physics [3]. The flow field will experience additional forces like Drag /Basset /Magnus /Saffman force and other gradient-related forces due to the appearance of solid particles[4]. Many experimental investigations show that some physical phenomena like particle-turbulence interaction, particle-mean fluid interaction, inter-particle collisions and particle-wall interaction can affect solid particles motion [5-7]. The physical properties of the particle such as the size, density and shape, and the boundary conditions including wall roughness can also influence flow behavior[8].

It is known that there are three basic theoretical methods available for gas-solid two phase flow. One is the single fluid model, second method is the two-fluid model and the third one is the discrete particle trajectory model[9]. Most of the properties are described as simple functions of particle/gas loading in the single fluid model. The two-fluid model describes each phase as a separate fluid with its own balance equations; in this approach each phase has its own velocity, temperature. The discrete particle trajectory model also treats the fluid phase as a continuum phase but the solid phase as single particles, where the particle motions is the result of the forces acting on particles. In general, the single fluid model is appropriate for initial theoretical studies[10].

There are many papers which focus on the two phase flow in pipes. Satishi Okuda and Woo Sik Choi have done the analyticl and experimental study gas-particle mixture flow in various types of convergent-divergent nozzle. They found the velocity of particle was influence by particle size[11]. C.R.Jackson and W.E.Lear have studied two phase flow using the shock tube[12], and their results show that the shocks influence the mixture temperature. Studies are conducted by R.Ishii and Y.Umeda on the flows of gas-particle mixtures in a

convergent-divergent nozzle[13]. They tried to predict the particle trajectories and erosion. In all of the above works the density variations in the flows were not captured because they have used simple incompressible models. The primary objective of this paper is hence, to develop an analytical model to estimate the effect of different nozzle exit pressure ratios, particle/gas loading and the particle diameter on supersonic two phase flow features. The single phase flow model is extended to solve the one-dimensional mass, momentum, and entropy equations for the steady pressure field. The mass flow, Mach number, thrust coefficient and pressure were computed and analyzed.

2. Formulation of Flow Field

An analytical model is developed to study the solid-gas suspension flow. The following assumptions are made in order to model the flow.

2.1 Assumptions

The particles used are very small, spherical in shape and of uniform size, they do not exchange mass with surroundings or react with each other.

(1) The specific heats of two phases are constant.

(2) The particles are uniformly dispersed in the gas, so that the value of temperature and velocity of both the phases are same.

2.2 Governing equations

The governing equations from [9] were used in present study are given as below.

$$\rho_{ds} = \rho_p \varepsilon \tag{1}$$

$$\rho_f = \rho_g (1-\varepsilon) \tag{2}$$

where: ρ_p is density of particle's material, ε is volume fraction, ρ_{ds} is dispersed density of the particles in suspension, ρ_g is density of gas phase, ρ_f is mass of gas in unit volume of the flowing suspension. Becasue the volume fraction is very small, less than 0.05, so that ρ_g almost equal to ρ_f .

The particle/gas loading (η) is constant defined by:

$$\eta = \rho_{ds} / \rho_f \tag{3}$$

The density of mixture (ρ_m) is defined by:

$$\rho_m = \rho_{ds} + \rho_f \tag{4}$$

The internal energy(U_{int}) of mixture is same as it for one-phase fluids :

$$U_{int} = \frac{C_v T}{\eta+1} + \frac{\eta C_s T}{\eta+1} \tag{5}$$

where: C_v is constant pressure specific heat of gas, C_s is specific heat of particles, T is temperature of mixture.

Similarly, the enthalpy (h_m) of mixture is:

$$h_m = u_{int} + \frac{p}{\rho_m} = \frac{C_p T}{\eta+1} + \frac{\eta}{\eta+1}\left(C_s T + \frac{p}{\rho_p} \right) \tag{6}$$

where: p is pressure of mixture. Cp is constant volume specific heat of gas,

The specific heat ratio of mixture ($\bar{\gamma}$) can get from Eq. 5 and Eq. 6:

$$\bar{\gamma} = \frac{\partial h_m / \partial T}{\partial u_{int} / \partial T} = \frac{\gamma\left(1 + \frac{\eta C_s}{C_p}\right)}{1 + \frac{\gamma \eta C_s}{C_p}} \tag{7}$$

where: γ is specific heat ratio of gas.

Assuming adiabatic flow, and by applying the first law thermodynamics, we get:

$$dQ = 0 = du_{int} - \frac{p d\rho_m}{\rho_m^2} \tag{8}$$

Rewriting the perfect gas law by mixture density, and using Eq. 5 :

$$(C_v + \eta C_s)\frac{dT}{RT} = \left(\frac{1}{1 - \frac{\eta\rho_m}{(\eta+1)\rho_p}}\right)\frac{d\rho_m}{\rho_m} \tag{9}$$

Integrating and substituting in Eq. 7 we get:

$$T\left(\frac{\rho_m}{1 - \frac{\eta\rho_m}{(\eta+1)\rho_p}}\right)^{-(\bar{\gamma}-1)} = C_1 \tag{10}$$

Using equations above and the perfect gas law by mixture density we get:

$$T\rho_g^{-(\bar{\gamma}-1)} = C_2 \tag{11}$$

$$p\rho_g^{-\bar{\gamma}} = C_3 \tag{12}$$

where: C_1, C_2, C_3 is the constant, it has defined in reference[9].

Although both the gas and the particles behave thermodynamically as a single fluid, physically only the volume occupied by the gas is available for accommodating changes in pressure.

The speed of sound in gas with suspended particles will be different from that of gas phase alone. Hence it is necessary to compare the changes in the speed of sound at different particle/gas loading of two phase flow. Through Prandtl's qualitative analysis for the mixture of snow or sand in air, it can be observed that the speed of sound in mixture is less than that of the prefect gas[8]. It is because the density of the compressible mixture is larger than that of the prefect gas. The speed of sound is given by definition:

$$a = \sqrt{\frac{\partial p}{\partial \rho}} \tag{13}$$

The speed of sound of two phase flow for isentropic conditions can be calculated by;

$$a_s = \left(\frac{\partial p}{\partial \rho_m}\right)^{\frac{1}{2}} \tag{14}$$

Using the above equations, it can get a relation for the speed of sound in gas-solid two phase flow in terms of the speed of sound in gas alone as shown below:

$$\frac{a_s}{a} = \left(1 + \frac{\eta\rho_g}{\rho_p}\right)\left(\frac{\bar{\gamma}}{\gamma(1+\eta)}\right)^{\frac{1}{2}} \tag{15}$$

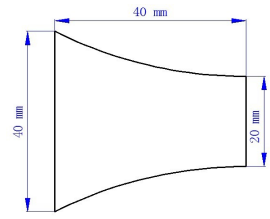

(a) Convergent Nozzle

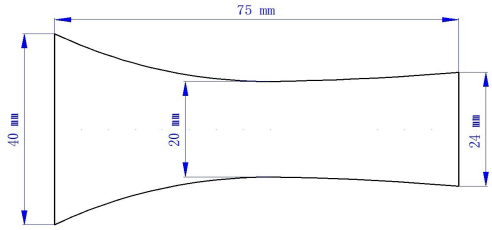

(b) Convergent-Divergent (C-D) Nozzle

Fig. 1 The Geometry and Dimensions of Nozzles

Table 1. Properties of Particle

C_s	ρ_p
880 J/kg/K	2719 kg/m^3

2.3 The Dimensions of Nozzles

The geometry and dimensions of convergent and convergent-divergent (C-D) nozzle are shown in Fig. 1. The inlet and throat diameters of both nozzles are same. The throat diameter is 20 mm.

2.4 Properties of Gas and Particle

The conditions and physical constants are listed in Table 1. The flow is in equilibrium. This paper employs on six kinds of particle /gas loading (η): 0, 0.1, 0.2, 0.3, 0.4 and 0.5, respectively.

3. Results and Discussion

Based on the equations above and the equations for single phase flow, the flow properties in the convergent nozzle and the C-D nozzle are calculated.

3.1 Analysis on two kinds of nozzles

At first, the results obtained for the convergent and the convergent-divergent nozzles were analyzed. The fluid is assumed to be consisting of only a perfect gas (particle/gas loading η =0).

Figure 2 shows the Mach number variation with the various back pressure ratios for the two nozzles. The curve for p_e/p_0=0.835 corresponds to the critical flow condition for C-D nozzle, and the flow is choked at the throat where the Mach number is unity. If the back pressure ratio less than 0.835, the flow will turn to supersonic in the downstream,

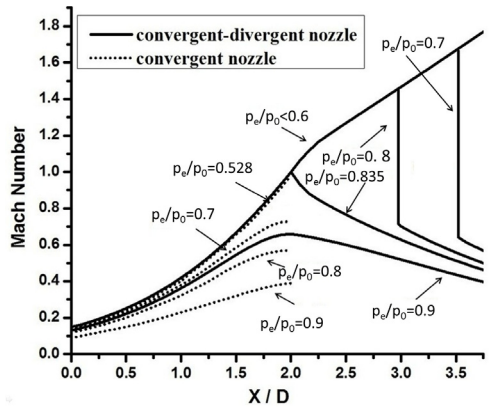

Fig. 2 Mach Number Distributions Along Centerline

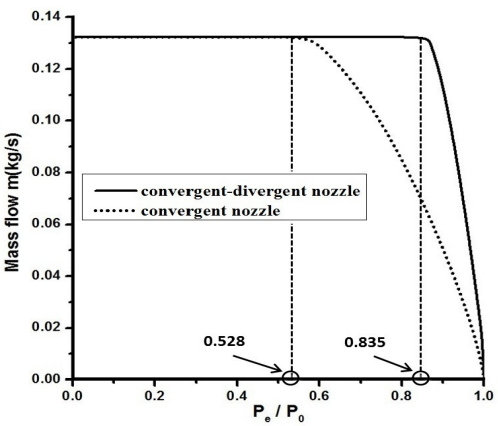

Fig. 3 Mass Flow Rate vs. Pressure Ratio

producing a shock wave in the divergent section. As back pressure decreases further, the position of shock will move towards the exit of nozzle. For the convergent nozzle, the critical flow condition curve is the same up to the halfway of C-D nozzle, and the back pressure ratio is 0.528.

The effects of the variation of the back pressures on mass flow rate of both nozzles are shown in Fig. 3.

3.2 Effect of particle/gas loading

The Fig. 4 illustrates the Mach number variations for single and two phase flow. Mach numbers are compared for two cases.

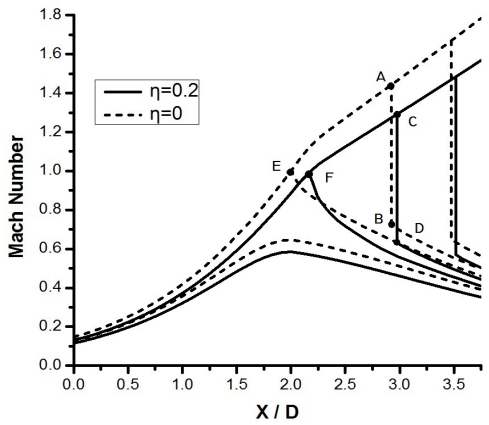

Fig. 4 Mach Number Distributions Along Centerline

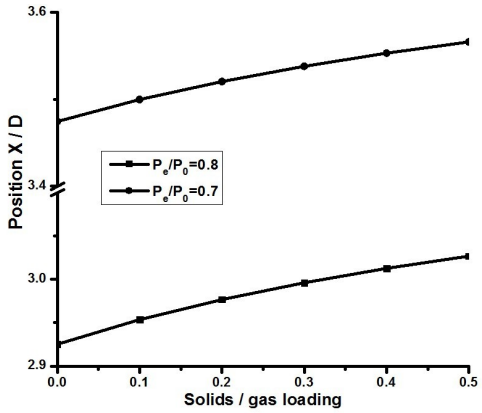

Fig. 5 Location of Shock Wave vs. η

The particle/gas loading is equal to 0 and 0.2, respectively.

It can be observed that the Mach number for single phase flow is larger compared to the two phase flow at same location. It is seems that as particle/gas loading increases, the Mach number of two phase flow is decreased. And the critical point (see point E and F in Fig. 4) moves towards downstream. This is due to the fact that, as particle/gas loading η increase, the density of mixture also increases; the mixture mass in unit volume becomes larger. For same p_e/p_0, the driving force will be same for all the cases, and hence the flow with lower particle/gas loading will get more acceleration compared to that with higher particle/gas loading.

This has an effect on shock wave behaviors. The reduction in Mach number across the shock for single phase flow (line AB in Fig. 4) will be larger compared to that across the shock of two phase flow (line CD in Fig. 4). The strength of the shock waves in both cases (P_2/P_1, where P_2 is the downstream static pressure and P_1 is the upstream static pressure of the shock wave), is calculated and found that the strength of shockwave is reduced when particle/gas loading η is increased. This means that the presence of solid particles will reduce the strength of the shock wave.

Figure 5 shows the effect of particle/gas loading on the location of the shock wave for two different pressure ratio, p_e/p_0 is 0.7, 0.8.

It clearly shows that the shock wave moves downstream when particle/gas loading η increases.

The variations of the mass flow rates of the two phase flow for various particle/gas loading is shown in Fig. 6. It is seen that chocking is attained gradually for higher particle/gas loading compared to the lower particle/gas loading and the critical pressure ratio is also decreased as shown in Fig. 7.

This is because of the velocity of mixture being decreased faster than the increase in density. Fig. 7 shows that as particle/gas loading η increases, the critical pressure decreases. However, the difference in the massflow rates is not large.

3.3 Effect of particle diameter

The effect of particle diameter is analyzed here. The previous assumption of uniform velocities for the particle and gas phase

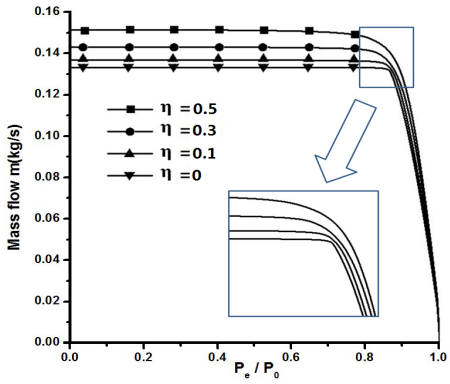

Fig. 6 Effect of η on Mass Flow Rate

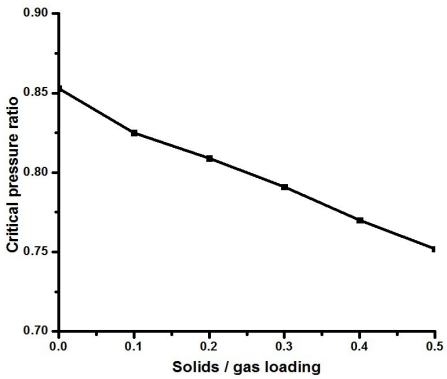

Fig. 7 Critical Pressure Ratio vs. η

becomes invalid here, as the gas phase velocity will be different from the particle velocity for larger particle diameters. This is because the slip velocity between gas and particles will be larger as the particle diameter increases.

The following equation is for particle velocity change in time [9]:

$$v_p \frac{dv_p}{dx} = \frac{3}{4} C_D \frac{\rho_g}{\rho_P d_P} (v_p - v_g)^2 \tag{16}$$

where: v_p is particle velocity, v_g is gas velocity, x is distance from nozzle inlet along x-axis, C_D is drag coefficient of particle, d_P is diameter of particle.

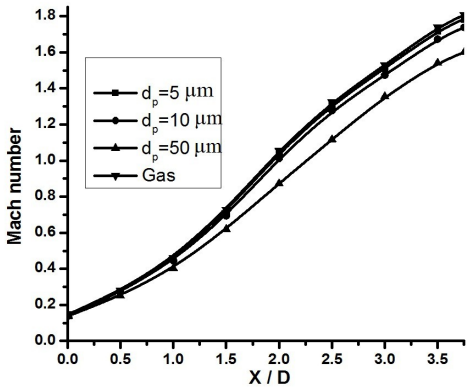

Fig. 8 Mach Number of Particle and Gas

C_D can be calculated by the Standard Drag Curves [14]:

$$C_D = \begin{cases} \frac{3}{16} + \frac{24}{Re_P} & Re_P < 0.01 \\ \frac{24}{Re_P}\left[1 + 0,1315 Re_P^{(0.82 - 0.051 g Re_P)}\right] & 0.01 < Re_P \le 20 \\ \frac{24}{Re_P}\left[1 + 0.1935 Re_P^{0.0305}\right] & 20 \le Re_P \le 260 \\ e^{1.6435 - 1.1242(1g Re_P) + 0.1558(1g Re_P)^2} & 260 \le Re_P \le 1500 \end{cases} \tag{17}$$

where: Re_P is Reynolds number of particle given by:

$$Re_P = \frac{\rho_g |v_g - v_P| d_P}{\mu} \tag{18}$$

where: μ is dynamic viscosity of gas given by Sutherland's law:

$$\mu = \mu_0 \left(\frac{T}{T_0}\right)^{\frac{3}{2}} \frac{T_0 + S}{T + S} \tag{19}$$

where: μ_0 is reference value of viscosity, T_0 is reference temperature; S is Sutherland constant. For air at moderate temperatures and pressures, μ_0 = 1.716*10^{-5} $Pa{\cdot}s$, T_0 = 273.11 K, S = 110.56 K.

The Particle Mach number variation for different particle diameters is shown in Fig. 8.

Flow loaded with different particle diameters has different slip velocities, when the flow is

accelerating. Larger the particle diameter is, greater the slip velocity is. The two phase flow with lower particle diameter (d_P =5 μm) shows almost same trend as that of single phase flow, as shown in Fig. 8. When the gas was flows through the divergent section, its velocity increases rapidly. This causes the particles also to speed up and the slip velocity between gas and particles become larger.

3.4 Thrust Coefficient

The thrust coefficient C_F can be calculated by [9]:

$$C_F = \sqrt{\gamma\left(\frac{2}{\gamma+1}\right)^{\frac{\gamma+1}{\gamma-1}}} \times \sqrt{\frac{2\gamma}{\gamma-1}\left\{1-\left(\frac{p_e}{p_0}\right)^{\gamma/(\gamma-1)}\right\}} + \sqrt{\gamma\left(\frac{2}{\gamma+1}\right)^{\frac{\gamma+1}{\gamma-1}}} \times \left(\frac{p_e}{p_0}-\frac{p_a}{p_0}\right) / \left[\left(\frac{p_e}{p_0}\right)^{1/\gamma} \sqrt{\frac{2\gamma}{\gamma-1}\left\{1-\left(\frac{p_e}{p_0}\right)^{\gamma/(\gamma-1)}\right\}}\right] \quad (20)$$

where: C_F is thrust coefficient, p_a is ambient pressure, p_e is outlet pressure of nozzle, p_0 is inlet pressure of nozzle.

Taking the derivative of Eq. 20 yields the following equation:

$$\frac{dC_F}{d(p_e/p_0)} = \sqrt{\gamma\left(\frac{2}{\gamma+1}\right)^{\frac{\gamma+1}{\gamma-1}}} \times \sqrt{\frac{\gamma-1}{2\gamma}}\left(\frac{p_e}{p_0}\right)^{-\frac{1}{\gamma}}\left(\frac{p_a}{p_e}-1\right) \times \left\{1-\frac{\gamma+1}{2}\left(\frac{p_a}{p_0}\right)\frac{\gamma-1}{\gamma}\right\}\left\{1-\left(\frac{p_e}{p_0}\right)^{\frac{\gamma-1}{\gamma}}\right\}^{-\frac{3}{2}} / \gamma \quad (21)$$

Equation 21 shows that thrust coefficient varies linearly with respect to inlet/outlet pressure ratio (p_e/p_0) and specific heat ratio (γ). When p_a/p_e < 1 the flow is "under expanded," the flow becomes "properly expanded," for p_a/p_e = 1 and when p_a/p_e > 1 the flow becomes "over expanded"[14].

The variation of thrust coefficient for different p_a/p_e (keeping p_a/p_0 as constant) is shown in Fig. 9. From the below figure it can be noticed that the variation in thrust coefficient can be divided into three sections.

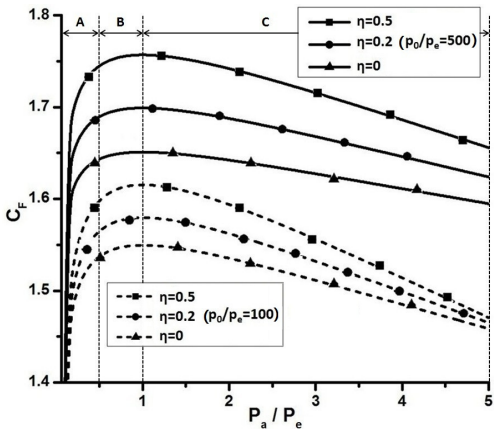

Fig. 9 C_F Variation with η

For low values of p_a/p_e ratio ($\leq$ 0.5) the thrust coefficient increases steeply as shown as section A in Fig. 9. Then the thrust coefficient shows almost a constant value as p_a/p_e value increases up to a critical point where the p_a/p_e value equals to 1 (Section B). At that point C_F becomes maximum (Right hand side of Eq. 21 becomes zero). There after the thrust coefficient decreases with increase in the pressure ratio (p_a/p_e). From Fig. 9 it can also be observed that for a constant value of p_a/p_e and p_0/p_e, the C_F increases as particle /gas loading η increases.

4. Conclusions

An analytical study is carried out to investigate the two-phase flow with particle /gas loading through typical convergent-divergent nozzles. The following conclusions are drawn from the analysis.

(1) The particles in the flow with lower particle/gas loading η will be more accelerated compared to that with higher particle/gas loading. The existence of

particles will reduce the strength of the shock wave in the nozzle.

(2) It is observed that the particle diameter affects the flow velocity adversely, the larger the diameter, the slower the flow will be. This is attributed to the larger slip velocities between the gas phase and solid phase when the particle diameter is large. The two phase flow with lower particle diameter has almost same trend as that of the single phase flow with ideal gas as working fluid.

(3) Depending on the ambient pressure, the thrust coefficient is found to be higher for larger particle/gas loading or inlet/outlet pressure ratio.

Acknowledgement

This work was supported by the National Research Foundation of Korea (NRF) grant funded by the Korea government (MEST) (2011-0017506)

References

1. J. H. Geng, H. Groenig, "Dust Suspensions Accelerated by Shock Waves," Experiments in Fluids, Vol. 28, 2000, pp.360-367
2. L. S. Fan, Chao Zhu, Principles of Gas-Solid Flows, Cambridge University Press, 1998
3. C. T. Crowe, D. F. Elger, J. A. Roberson, Engineering Fluid Mechanics, Wiley-Vch Verlag GmbH & Co. KGaA, 2008
4. M. A. F. Kendall, "The Delivery of Particulater Vaccines and Drugs to Human Skin with A Practical Hand-held Shock Tube-based System," Shock Waves, Vol. 12, Issue 1, 2002, pp.23-30
5. M. V. Protasov, A. Yu. Varaksin, T. F. Ivanov, A. F. Polyakov, "Experimental Study of Downward Turbulent Gas-Solid Flow in Narrow Pipe," 4th Int. Symp. on Turbulence, Heat and Mass Transfer, 2003
6. Y. M. Lee, R. A. Berry, "Analysis of The Two-Phase Flow in A De Laval Spray Nozzle and Exit Plume," Journal of Thermal Spray Technology, Vol. 3, No. 2, 1994, pp.179-183
7. H. Staedtke, Gasdynamic Aspects of Two-Phase Flow, Wiley-Vch Verlag GmbH & Co. KGaA, 2006
8. S. Chellappan, G. Ramaiyan, "Experimental Study of Design Parameters of a Gas-Solid Injector Feeder," Power Technology, Vol. 48, Issue 2, 1986, pp.141-144
9. R. G. Boothroyd, Flowing Gas-Solid Suspen- sion, T&A Constable Ltd., 1971
10. R. G. Maev, Volf Leshchynsky, Introduction to Low Pressure Gas Dynamic Spray, John Wiley & Sons., 2009
11. S. Okuda, W. S. Choi, "Gas- Particle Mixture Flow in Various Types of Convergent-Divergent Nozzle", Journal of Chemical Engineering of Japan, Vol. 11, No. 6, 1978, pp.432-438
12. C. R. Jackson, W. E. LEAR, "Generalized Shock Wave Analysis of Two-phase Flow," Mechanics Research Communications. Vol. 25, No. 6, 1998, pp.613-622
13. R. Ishii and Y. Umeda, "Nozzle Flows of Gas-Particle Mixtures," Phys. Fluids, Vol. 30, No. 3, 1987, pp.752-760
14. S. T. Yao, L. J. Zhong, Foundation of Gas-Solid Two-phase Flow of Turboma-chinery, China Machine Press., 1994